ELSEVIER

PII: S0032-3861(97)0058-X

Polymer Vol. 38 No. 20, pp. 5125–5135, 1997

0032-3861/97/$17.00 + 0.00

Solubility of erucamide (13-*cis*-docosenamide) in isotactic poly(propylene) and thermal behaviour of their blends

I. Quijada-Garrido, J. M. Barrales-Rienda* and J. M. Pereña
Departamento de Química-Física de Polímeros, Instituto de Ciencia y Tecnología de Polímeros, C.S.I.C. Juan de la Cierva, 3, E-28006 Madrid, Spain

and G. Frutos
Departamento de Estadística e Investigación Operativa, Facultad de Farmacia, Universidad Complutense, E-28040 Madrid, Spain
(Revised 11 December 1996)

Differential scanning calorimetry studies, made on blends prepared by mixing in the melt, have demonstrated that crystallization of erucamide (13-*cis*-docosenamide) $[H_3C-(-CH_2-)_7-HC=CH-(-CH_2-)_{11}-CO-NH_2]$/ isotactic poly(propylene (i-PP) blends results in separate crystals of the two components, rather than cocrystallization. For low content erucamide blends (less than 29%), two melting peaks for erucamide have been observed. They have been assigned to: i) erucamide crystals situated in the external surfaces of the i-PP and located forming globules, droplets or inclusions whose melting point appears at the higher temperature (Erucamide I); ii) erucamide crystals forming crystalline microdomains of erucamide, located either within the amorphous region of spherulites and/or in the amorphous regions which surround the spherulites (Erucamide II). The enthalpy of these crystals located in these regions, i.e. in the amorphous region of the spherulites and/or their surroundings, has been estimated. A good linear correlation has been found between the solubility of erucamide crystals in the amorphous region of i-PP spherulites and/or the surrounding region of the spherulites and their apparent melting enthalpy. Spherulite radial growth rates, G, for the different blends are lower than for the pure i-PP. They show a characteristic dependence on the erucamide content in the blend. This behaviour is in agreement with theoretical predictions for crystallization in immiscible blends. An additional feature, as an unambiguous test of the incompatibility, is the poor interfacial adhesion, which has been made clear from the large voids left on the fracture surface where the erucamide globules have separated from the matrix and from the smooth surfaces of the exposed erucamide globules. A model is proposed for erucamide/i-PP blends, which is able to explain quantitatively in detail all the thermal and morphological experimental data. © 1997 Elsevier Science Ltd.

(Keywords: erucamide (13-*cis*-docosenamide); isotactic poly(propylene); blends)

INTRODUCTION

Recent concerns about the development of films, for food packaging and some other packaging applications, with slipping and antiblocking properties have made the study of additives promoting these properties a matter of great importance to the polyolefin film industry. Slip agents have some properties, such as: (i) decreasing the coefficient of friction; (ii) reducing blocking; (iii) reducing chill-roll sticking; (iv) increasing dispersion and preventing plate-out in pigmented materials[1]. To know the behaviour, and for the design of new slipping and antiblocking additives, the most important basic information is that on the solubility and diffusion of these additives in polyolefins. In this paper we present the results of a recent study of erucamide (subsequently referred as ERU) solubility in isotactic poly(propylene) (i-PP) and its dependence on concentration and temperature. The solubility of additives in polymers determines the state of the additive in a processed sample, and the mechanisms by which it may diffuse through the polymer and be lost[2]. Our concurrent study of the rate of erucamide diffusion in i-PP is being published separately[3]. Erucamide has, to a great extent, replaced the use of oleamide, because of its higher melting point and higher thermal stability[4].

Solubility of small molecules in polymers is determined by the free volume of the polymer, the size and shape of the additive, and the polymer–polymer as well as the polymer–additive thermodynamic interactions[5–9]. The problem of interaction between additives and i-PP chains is still not very well understood[10–12]. However, additives seem to be placed in the amorphous phase in spite of their crucial influence on the formation of the crystalline phase of i-PP[13]. In polymer–diluent systems as a general rule, as the crystal grows, diluent is rejected from the growing crystal, leading to a high concentration of the diluent at the crystal–melt interface. The diluent attempts to diffuse away from the growth front to the amorphous polymer–diluent region. However, if the

* To whom correspondence should be addressed

concentration at the interface remains high because of poor diffusion, the growth rate is not constant and the growth process is transport-controlled[14,15]. Information about the local incompatibility of the two components can be obtained from the determination of the glass transition and some other relaxations[16].

Results and conclusions about the behaviour of polymer–additive blends are very scarce. However, conclusions drawn from incompatible polymer blends can tell us about the origin of changes in the crystallization pattern, whether they are due to structural, equilibrium thermodynamic or kinetic effects. Among the most significant effects, there have been reported the induction of specific crystal modifications[17], the rejection, engulfing, and deformation of the dispersed component by the growing spherulites of the matrix material[18,19], and the nucleation at the interface[18,20]. Polymer blends containing one of their components as finely dispersed globules or droplets may exhibit the well known process of fractionated crystallization, which is originated in the primary nucleation of isolated particles in the melt by units of different nucleating species[21–23]. Tang and Huang[24] have demonstrated that the phenomenon of fractionated crystallization is related to the volume fraction of the dispersed phase and the matrix in the case of i-PP/nylon 6 blends.

EXPERIMENTAL

Materials

Poly(propylene) (i-PP). Hostalen PPN 1060 (Hoechst Ibérica, S.A., Barcelona, Spain) free-additives isotactic poly(propylene) of nominal melt index (MI)= 9 g per 10 min at 230°C and 5 N, nominal density at 23°C of 0.905 g cm^{-3} and 54.2% of crystallinity, was supplied by Disper, S.A., Sant Andreu de la Barca (Barcelona, Spain).

Erucamide (13-cis-docosenamide) [$H_3C-(-CH_2-)_7-HC=CH-(-CH_2-)_{11}-CO-NH_2$]. A commercial sample of Armoslip (Exp) Beads with 96.5% purity, which has been used in blends and as standard material for capillary gas-liquid chromatography (c.g.l.c.) tests and calibrations, was kindly supplied by Akzo Chemicals, S.A., División Química (El Prat de Llobregat, Barcelona, Spain) and used as received. Nominal melting point 80°C.

Stearic acid. Stearic acid, 99% purity (Fluka Chemie, A.G. Buchs, Switzerland), employed as an internal standard to estimate erucamide content in blends by c.g.l.c., was used as received.

Chloroform. An analytical grade chloroform (Quimicen, S.A., Madrid, Spain) needed for Soxhlet solvent extraction was used as received.

Methods

^{13}C Nuclear magnetic resonance. Isotactic pentad fraction (IPF = 0.92) was evaluated by ^{13}C nuclear magnetic resonance (n.m.r.) spectroscopy by using a Bruker AC300 spectrometer operating at 75.47 MHz and 7.046 T. The spectrum was measured in 1,3,5-trichlorobenzene solution at 393 K using $Cl_4C_2D_2$ as internal standard.

Molecular weight distribution. Molecular weight averages and polydispersity factor (molecular weight averages are in daltons (g mol^{-1})), $\bar{M}_n = 9.79 \times 10^4$; $\bar{M}_w = 4.35 \times 10^5$; $\bar{M}_z = 3.34 \times 10^6$; $\bar{M}_v = 3.18 \times 10^5$ and $\bar{M}_w/\bar{M}_n = 4.44$; were estimated by size exclusion chromatography (s.e.c.) with a Waters ALC/GPC 150 gel permeation chromatograph (g.p.c.) at 140°C in 1,3,5-trichlorobenzene, following standard techniques.

Preparation of mixtures. Blends of erucamide/i-PP having the compositions shown in *Table 1* were prepared

Table 1 Melting points T_m, and apparent melting enthalpies, ΔH_m, of i-PP and erucamide (ERU I and ERU II) and a series of their blends measured by d.s.c. at a heating rate of $R_H = 20.0$ K min^{-1}

						Crystalline erucamide			
		i-PP				Erucamide I (External)[b]		Erucamide II (Internal)[c]	
Sample	Composition erucamide (wt%)	T_g (K)	T_m (K)	ΔH_m (J g^{-1})	X_c^a (%)	T_m (K)	ΔH_m (J g^{-1})[d]	T_m (K)	ΔH_m (J g^{-1})[e]
1	0	268	438	92	50.0	–	–	–	–
2	2	268	437	96	52.1	352	4	337	70
3	4	265	436	105	57.0	350	3	335	83
4	8	269	435	100	54.3	348	4	336	75
5	16	267	433	103	55.9	350	24	336	81
6	29	–	431	103	55.9	346	96	342	84
7	45	–	432	110	59.8	353	128	–	–
8	47	–	432	97	52.7	353	124	–	–
9	85	–	432	102	55.4	354	122	–	–
10	100	–	–	–	–	360	144	–	–

[a] $X_c = (\Delta H_m/184.1) \times 100$
[b] External, as globules or droplets in the polymeric matrix (Erucamide I)
[c] Internal, in the amorphous region of i-PP spherulites (Erucamide II)
[d] This melting enthalpy does not really correspond with the melting enthalpy of pure Erucamide I, but with the enthalpy estimated from the higher temperature endotherm and the total amount of erucamide in the sample
[e] The amount of erucamide in the amorphous i-PP spherulites has been calculated by difference between the total amount of erucamide determined by means of c.g.l.c. analysis, as has been indicated in the text, and the erucamide content on the external surface of the i-PP matrix as globules or droplets

as follows: first, blends of erucamide/i-PP were prepared by dry-mixing of erucamide granules and i-PP pellets. An antioxidant additive, IRGANOX 1076 (Ciba-Geigy, Basel, Switzerland) was added in a small quantity (less than 0.1% w/w polymer) to protect against thermal oxidation and degradation. The dry-mixed blends were then mixed by mechanical blending in a home-made Brabender mechanical blender equipped with a mixing head capacity of 50 ml, previously heated to 200°C and fully fluxed with nitrogen as a purging gas for 5 min. Mixing occurred at 50 rpm, using the roller blades recommended for high shear application. The torque was recorded during the blending time (10 min). The molten blends were removed from the mixing chamber and immediately quench-cooled in a water–ice mixture. Films were made by compression moulding at 200°C, a temperature exceeding the melting point of i-PP as well as of erucamide, using a Collin press Model 300, with the following temperature and pressure programs applied to the plates. Firstly, a pressure of 5 bar was applied during 3 min, immediately after, the pressure was elevated to 10 bar during 3 min, and in a third stage the pressure was maintained at 35 bar during 5 min. Finally, the sample was quenched between the two plates refrigerated with cool water (10°C) at a pressure of 35 bar during 3 min. Samples of unblended i-PP and erucamide were submitted to the same treatment, namely, antioxidant additivation, the same time was used for the blending, and the same thermal history treatment and quantitative analysis for i-PP and erucamide contents. For crystallization kinetic experiments we have also prepared a blend with a 68 wt% erucamide content. Its description has not been included in *Table 1*. The composition for each one of the blends was estimated as follows.

Measurement of i-PP and erucamide contents. The general analytical approach chosen was to extract the blends. Some other details and procedures have been given elsewhere[3]. For erucamide content a method based on c.g.l.c. was followed. We used a procedure reported by Brengartner[25] for the separation of fatty acid amides using glass capillary columns. Some other details and descriptions of the chromatographic equipment and techniques have been given elsewhere[20]. Erucamide percentages for blends are included in the second column of *Table 1*.

Preparation of mixtures from additives-free films. As we will see subsequently, in order to get additional information, by means of the calorimetric behaviour, on the location of the erucamide molecules within the amorphous regions of spherulites and/or the amorphous regions surrounding the spherulites, we have additionally prepared some other erucamide/i-PP blends.

A second series of blends was artificially prepared as follows: round discs of diameter 2 cm and thickness 1 mm were cut off from an unadditivated i-PP film. They were placed into a closed system in melt erucamide, held at a constant temperature of 100°C. After 1 and 5 days, two of these discs were taken out separately and immersed into a large quantity of dichloromethane at room temperature for a few seconds, in order to cool and to remove roughly the excess amounts of erucamide adhered to the surface of the i-PP disc. The disc was then wiped and polished on filter paper to remove the superficial erucamide. The surface was controlled by optical microscopy. Additive concentration within the now additivated i-PP film was determined as before.

Following the same purpose a third type of artificial mixture was prepared. The method for the preparation of this sample was the same as in the previous paper[3]. A uniform disc of the i-PP, which did not contain any diffusant, was placed face-to-face between two additive source plates which contained diffusant erucamide molecules at a concentration of 6%. The whole system was put into a diffusion cell and kept at a temperature of 75°C for a period of 12 days. The diffusion process was terminated after the additive concentration in the film reached the equilibrium concentration. Additive concentration was determined as before. All these samples and their thermal characteristics are described in *Table 2*.

Density measurement and degree of crystallinity. The density of pure i-PP, measured by means of a floating and pycnometric technique, was 0.898 g cm^{-3} which corresponds[26] (with $\rho_a = 0.850\,g\,cm^{-3}$ and $\rho_c = 0.943\,g\,cm^{-3}$ and degree of crystallinity, $X_c = [\rho_c/\rho] \cdot [\rho - \rho_a/\rho_c - \rho_a] \times 100\%$), to a degree of crystallinity of 54.2%. This value agrees quite well with that calculated from differential scanning calorimetry (d.s.c.) measurements of 50.0% on a sample with almost the same thermal history, as can be seen in *Table 1*.

Differential scanning calorimetry. D.s.c. measurements were carried out under a blanket of N_2 with a Perkin-Elmer DSC-7 connected to a cooling system. In

Table 2 Thermal properties of erucamide located within the amorphous regions of i-PP spherulites and/or the surrounding amorphous regions of spherulites (ERU II)

			ERU II		
Sample	Preparation procedure	Time (days)	T_m (K)	$\Delta H_m \pm 10$ (J g^{-1})	Composition erucamide (ERU II) (wt%)
(a)	From diffusion experiment at 348 K (For protocol description see ref. 23)	12	~323	77	1.2
(b)	By i-PP film immersion in melt erucamide at 373 K	5	333	94	2.4
(c)		1	337	88	2.4
(2)	By erucamide/i-PP melt dry blending after cooling to room temperature		337	68	2
(3)		0	335	91	4
(4)			333	65	8

order to destroy the self-seeding nuclei in the components and to submit all the samples to the same thermal history, the samples were preheated for 15 min at 200°C. Then the crystallization and reheating runs were performed at a standard rate of 20.0 K min^{-1}. Typical sample weights ranged from 5 to 10 mg.

The melting temperatures were obtained from the endothermic peaks maxima. The apparent melting enthalpy ΔH_m of unadditivated i-PP, pure erucamide and their blends were calculated from the area of the d.s.c. endothermic peaks, by using the indium melting enthalpy, $\Delta H_m(\text{indium}) = 28.46\ J\ g^{-1}$ as a standard. A detailed analysis of some of these endothermic peaks will be shown later on. The crystalline and amorphous weight fractions, after weight normalization, were calculated from the following relations: $w_c = \Delta H_m/\Delta H_{i-PP}$ and $w_a = (1 - w_c)$, where $\Delta H_{i-PP} = 184.1\ J\ g^{-1}$ is the melting enthalpy per gram of 100% crystalline i-PP[27].

The actual value for the glass transition temperature, T_g ($T_{1/2}$) has been estimated following a criterium given some years ago by Barrales-Rienda *et al.*[28] to determine the T_g from $C_p - T$ traces obtained by d.s.c. $T_{1/2}$ is the temperature at the midpoint of the line drawn between the temperature of intersection of the initial tangent with the tangent drawn through the point of inflection of the trace and the temperature of intersection of the tangent drawn through the point of inflection with the final tangent. The estimated values for the glass transition are given in the third column of *Table 1*. They do not seem to depend on blend composition.

Wide angle X-ray scattering. X-ray diffraction patterns of samples at wide angles (wide angle X-ray scattering, WAXS) were taken by using a Geiger counter X-ray diffractometer, made by Philips, that used Ni-filtered Cu–Kα radiation. The generator operated at 40 kV and 25 mA. The intensities were recorded through the range of 3 to 35 2θ degrees.

Isothermal crystallization. The spherulitic growth rate of i-PP and its blends with erucamide has been studied by means of optical polarizing microscopy. Samples were prepared by melting, on a controlled hot plate, a few milligrams of the polymer or blend between a microscopy slide and a cover glass. Pressure was applied to the cover glass to obtain samples having a thickness of around 10 μm, as measured by micrometry. Crystallization was observed between cross-polaroids at a 80 × magnification with a Carl Zeiss (Jena, Germany) Model Amplival POL-D microscope, equipped with a Mettler hot stage model FP 82 HT, having an accuracy of ±0.2°C controlled with a central processor Mettler FP 80 HT. We followed more or less the same protocol as that given by St Jean *et al.*[29] to prepare the samples for thermo-optical analysis. In the present series of experiments, i-PP and its blends were isothermally crystallized from the melt at 403, 404, 406, 408, 411, and 412 K. These temperatures are well above the melting temperature of the erucamide. Therefore, erucamide must remain in the melt phase during the crystallization of i-PP. The radii of the spherulites were measured with a calibrated photographed scale. The slope of the linear plot of the radius as a function of time gave the radial growth rate, G.

Scanning electron microscopy. Bars of 2 × 4 × 20 mm^3 were prepared by moulding compression. These undeformed specimens were cryogenically fractured perpendicular to the compressed-moulding direction after submersion in liquid nitrogen for 30 min. The fracture surfaces were coated with a 60 Å layer of gold–palladium, in order to make them electrically conductive and to observe the domain morphology. This was done by using a high resolution electron scanning microscope ISI-DS 130 operated at 20 kV.

RESULTS

Differential scanning calorimetry

Some of the present authors[30] have stated in a detailed study carried out previously that erucamide does not reveal any crystal to crystal transition when it is submitted to different thermal histories, rates of heating, rates of cooling, quenching, annealing, etc.

Figure 1 illustrates the melting behaviour of i-PP, pure erucamide and some of their blends, from 300 K to 473 K. Moreover, looking for T_gs, they were registered at the same rate but from 233 K to 300 K. It is very easily noted that for blends of low erucamide content, as is shown in *Figure 1*, we can appreciate in their d.s.c. traces two separated melting endotherms, around 340 and 355 K, which have been summarized in the seventh and ninth columns of *Table 1*. The endotherm which appears at the higher temperature, namely at 355 K, is a sharp peak, but because of its shape and location it is the same

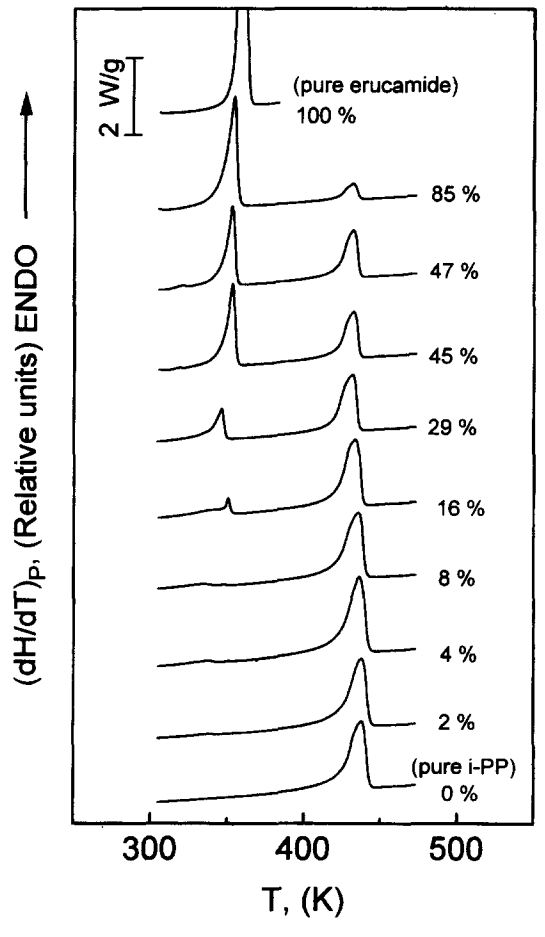

Figure 1 D.s.c. traces recorded during a heating cycle at a nominal heating rate of $R_H = 20.0\ K\ min^{-1}$, for i-PP and a series of erucamide/i-PP blend samples. Their compositions are indicated

as that which appears in the sample of pure erucamide (100% eru content), as can be seen in *Figure 1*. In *Figure 2* we have produced a plot of the apparent melting enthalpy corresponding to this endotherm, which has been estimated by taking into account the overall content of erucamide in each sample. As can be seen, the apparent melting enthalpy increases to the utmost the enthalpy of pure erucamide for samples within a higher content of erucamide. The sigmoidal shape of *Figure 2* gives us cause to suspect that really the 355 K endotherm does not correspond to the global erucamide content, but only to a part of it which adopts a structure similar to that found in the pure compound, whereas the remaining erucamide has undergone some change within its original crystalline structure.

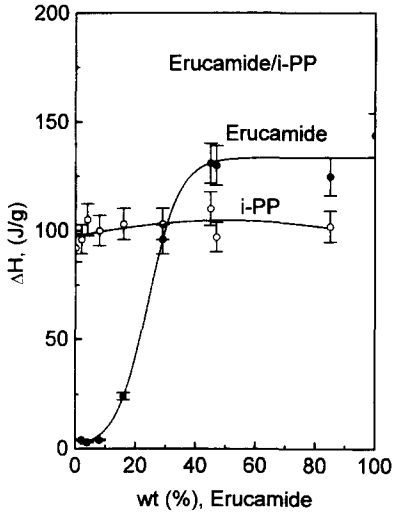

Figure 2 Apparent melting enthalpies ΔH_m of pure i-PP and pure erucamide and these two compounds in their erucamide/i-PP blends determined by d.s.c. as a function of erucamide content in the blends. Actually the plot of the apparent melting enthalpy of erucamide really represents the endothermic effect due to Erucamide I divided by the whole content of erucamide (Erucamide I + Erucamide II)

For low erucamide content samples, the curves have been resolved by means of a curve deconvolution method, as is shown in *Figure 3*. Peaks appearing at the higher temperature side have been assigned, which we will designate from now on as the external erucamide (Erucamide I, subsequently referred as ERU I), i.e. the erucamide supported on the external surface of i-PP as globules, or droplets. Those which appear at the lower temperature side have been assigned to crystalline erucamide located in the amorphous regions of i-PP spherulites and/or in the amorphous regions which surround the spherulites (Erucamide II, subsequently referred to as ERU II), i.e. erucamide located within the amorphous regions of spherulites. The amount of erucamide located on the external i-PP surface as globules, droplets or inclusions has been estimated from the area of the d.s.c. endothermic peak which appears at the higher temperature, using the melting enthalpy of pure erucamide as (ΔH_m (ERU I) = 144.2 J g^{-1}). The amount of erucamide in the amorphous part of i-PP spherulites and/or in the regions which surround the spherulites, has been calculated by the difference between the total erucamide content used to prepare each blend and the amount supported on the external surface as globules or droplets of i-PP previously estimated. In *Figure 4*, we have plotted the area of the peaks appearing at the lower temperature, against the respective amount of erucamide. This yields quite a good straight line, showing that there exists a very good correlation between the area of this endotherm and the content of ERU II. On the other, we can observe (see *Figures 1* and *3*) that at the very beginning the blends contain almost only i-PP, and practically all the erucamide is located in the amorphous region of i-PP spherulites and/or in the amorphous regions which surround the spherulites. However, as the erucamide content is increased, the relative fraction of amorphous i-PP decreases, so the ratio of internal to external erucamide gets lower and the amount of erucamide in the amorphous region of the spherulites and/or the amorphous regions which surround the

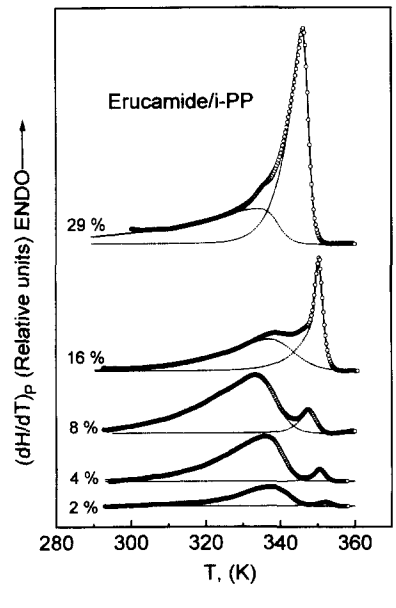

Figure 3 Deconvolution in the erucamide region of some of the d.s.c. traces of a series of erucamide/i-PP blends, as shown in *Figure 1*. Their compositions are indicated

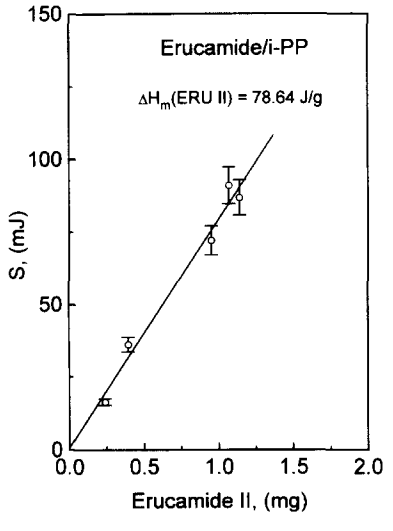

Figure 4 Plot of the area of the melting endotherms due to the erucamide which is located in the amorphous regions of the i-PP spherulites and/or in the surrounding regions of spherulites (Erucamide II) against the erucamide content in the amorphous regions of the i-PP spherulites and/or in the surrounding regions of spherulites (Erucamide II) in erucamide/i-PP blends. They have been calculated as indicated in the text

spherulites decreases. Nevertheless, the ratio of energy to effective weight of erucamide must remain constant, and this fact is confirmed in the plot given in *Figure 4*. The slope of this plot affords a value of $78.6\,J\,g^{-1}$ for the apparent melting enthalpy for this crystalline phase of ERU II, since at this point we do not know what type of erucamide is located. From this value, which is almost a half of the value of $144.2\,J\,g^{-1}$ for the erucamide which we have termed as external erucamide, namely, which is in the form of globules or droplets, we may conclude that erucamide in the amorphous regions of i-PP spherulites and/or in the interphase which surround the spherulites, presents a quite different crystalline structure than that of the globules or droplets which we have called external erucamide. But before drawing conclusions, we must be sure that either the amorphous fraction or the crystalline fraction of our blends do not change with the erucamide content. It suggests that the amorphous fraction of i-PP available for erucamide molecules remains constant all over the composition range, as we will see later.

Figure 5 shows the d.s.c. traces of erucamide/i-PP blends prepared by immersion and diffusion. Values for the apparent melting enthalpies are given in *Table 2*, where the enthalpies of melting for samples prepared by melt blending have also been included for comparative purposes. Therefore, we have three different types of blends with a very low erucamide content (<8%), which has been prepared by means of three quite well differentiated procedures. Notwithstanding this, in two of these three cases, erucamide is clearly and unequivocally located in the amorphous regions of i-PP spherulites, because in these two cases erucamide is introduced by diffusion of erucamide from a source (diffusion experiment) or by immersion of a virgin film into melt erucamide (immersion experiment). Therefore the melting maxima belong to the erucamide located in the amorphous regions. Similarly, for the samples prepared by melt blending of erucamide and i-PP with a low erucamide content, where we cannot appreciate any type of erucamide as globules. We can also appreciate that erucamide melts at the same temperature as erucamide in mixtures prepared by diffusion and immersion experiments. We can conclude that in the three cases we have erucamide crystals located in the amorphous regions of spherulites with identical melting points and apparent melting enthalpy, which does not correspond either with the melting point of pure erucamide or with the erucamide located at the external surface of the polymeric matrix as globules in blends prepared by melt blending. The apparent melting enthalpy for each one of these low content erucamide samples is in all cases proportional to their erucamide content estimated by chromatography. From the apparent melting enthalpy data obtained from samples prepared by immersion or diffusion, and the respective values obtained for melt blending samples, as depicted in *Figure 5* and gathered in *Table 2*, we can consider as precise the assignation we have made before for the endothermic peak, which appears at a lower temperature in the d.s.c. traces given in *Figure 3*. This second crystalline form of erucamide will be henceforth definitively designated as ERU II.

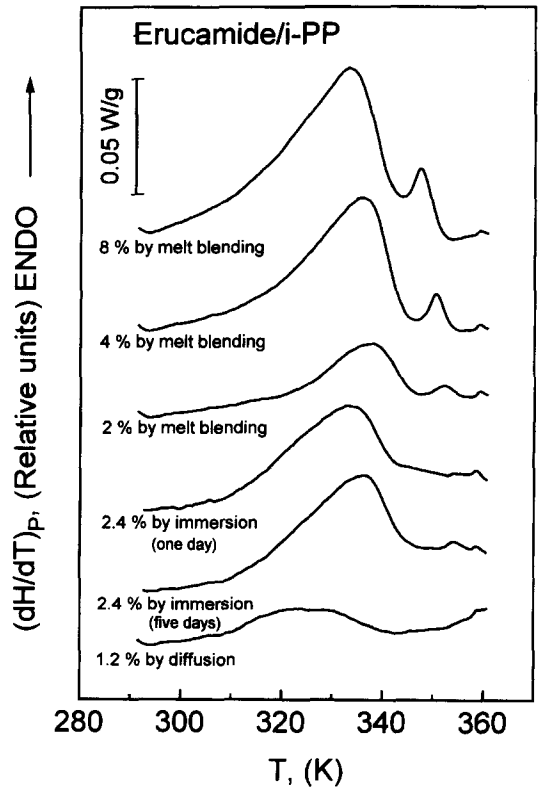

Figure 5 D.s.c. traces recorded during the first heating cycle at a nominal heating rate of $R_H = 20.0\,K\,min^{-1}$ for a series of erucamide/i-PP blends prepared as indicated. Details on their preparations are described in the text

Glass transition temperature

From the d.s.c. traces given in *Figure 1* we have estimated the value of the T_g of unadditivated i-PP, and its blends with erucamide. T_g values, estimated as described in the Experimental section are in the third column of *Table 1*. As can be seen, the value of T_g does not seem to be dependent on blend composition.

Crystallinity

Values for the i-PP crystallinity in erucamide/i-PP blends are given in the sixth column of *Table 1*. As can be

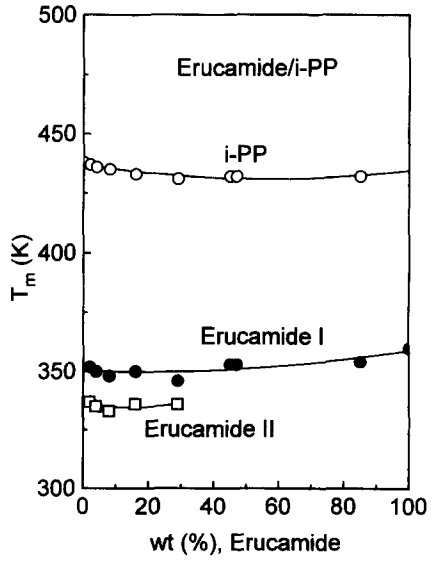

Figure 6 Plot of melting temperatures, T_m, of i-PP, erucamide and erucamide/i-PP blends as a function of erucamide concentration (%), determined by d.s.c. from experimental data given in *Figure 1*, and from their deconvoluted curves given in *Figure 3*

very easily seen, the degree of crystallinity does not seem to depend appreciably on the erucamide content. For this reason we can conclude that the amorphous i-PP fraction available for our additive is constant through all the range of composition studied. However, we cannot decide whether this last erucamide, that we have already called ERU II, is situated at the region which surrounds the spherulites, or if it is dispersed in the amorphous region of spherulites, forming in both cases crystalline microdomains. In this respect, it is now well established that long chain molecules (additives or impurities), as some authors[31–35] have demonstrated, are largely rejected by the growing crystallites, and are accumulated in the noncrystalline regions, either between radial crystalline fibrils or between the spherulites and a dip at the spherulite centre.

Experimental melting points, T_m, and apparent melting enthalpies, ΔH_m, for each one of the components and the crystalline phases in the blends have been collated in *Table 1*. Melting points are plotted in *Figure 6*, as a function of the percentage of erucamide content in blends.

Wide angle X-ray scattering

Figure 7 shows the WAXS curves for erucamide, i-PP, and their eucamide/i-PP blends. As can be observed, the crystallization of the components in the blends takes place separately, since in the spectra of the blends, the characteristic diffraction maxima only appear due to each one of the pure components. Thus, for instance, i-PP crystallizes in the crystalline α monoclinic. These maxima agree with those given by Martuscelli *et al.*[36], namely (110) at 14.4 2θ; (040) at 17.2 2 θ; (130) at 18.8 2θ; (111) at 21.4 2θ; (131) and (041) at 22.1 2θ and (060) at 25.7 2θ. In some of the blends there appears a maximum due to a small proportion of the crystalline β hexagonal form, (300) at 16.3 2θ. Maxima of diffraction for pure erucamide and pure i-PP are indicated in *Figure 7*. Wenig and Fiedel[37] have observed in i-PP/*trans* polyoctenyle (TOR) mixtures a small quantity of i-PP crystallized in the crystalline β hexagonal form. This fact has also been observed by Wenig and Wasiak[38] in the case of mixtures of i-PP and an ethylene–propylene elastomer.

On one hand, the maxima of diffraction corresponding to erucamide do not appear very clearly, up to a blend with 29% eru content. On the other hand, the relative proportion of the amorphous halo is also increased up to this sample[39]. However, from the data furnished by the d.s.c. experiments, it was not possible to detect any noticeable regular change in this zone for the i-PP crystallinity (see sixth column of *Table 1*). This may be due to the fact that the diffraction maxima of erucamide are smeared because the number and size of erucamide crystals may be too small to contribute to the WAXS spectrum, causing the erucamide intensity to disappear into the background.

Isothermal crystallization

The aim of this experiment has been to analyse the effect that an incompatible additive such as erucamide has on the isothermal crystallization kinetics of i-PP in erucamide/i-PP blends.

Few studies of polymer crystallization from mixtures with low molecular weight solvents, diluents or plasticizers over wide concentration ranges have appeared in the literature. Most of these studies have concentrated on developing crystallization kinetic equations[40,41] and describing the effect of dilution on the polymer crystallization rate[42,43] and crystal morphology[44]. Keith and Padden[45,46] proposed that diluent addition reduces polymer nucleation density and increases polymer mobility. Consequently, crystallization rate and spherulite morphology were significantly changed with i-PP crystallized in the presence of low molecular weight atactic polypropylene[45–47].

The measured spherulitic radii were plotted against time, t. A plot of the spherulitic radius as a function of the crystallization time is given in *Figure 8*. The growth rate was taken as the slope of the linear plot. In all cases a linear regression slope with correlation coefficient ≥ 0.99 was obtained. The growth rates which were extracted from the linear plot of the radius vs time are given in

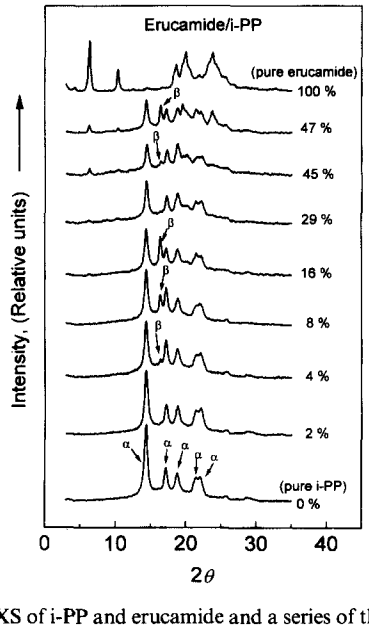

Figure 7 WAXS of i-PP and erucamide and a series of their erucamide/i-PP blends. Their compositions are indicated

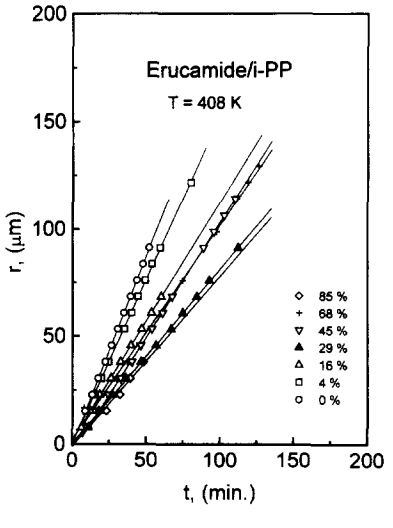

Figure 8 Effect of erucamide content in erucamide/i-PP blends on spherulite growth rate of i-PP and of i-PP in erucamide/i-PP blends at 408 K estimated by polarizing optical microscopy. Their compositions are indicated. The sample with a 68 wt% erucamide content has been specially prepared for crystallization kinetic experiments

Figure 8. Spherulitic growth rates, measured at several temperatures, are listed in *Table 3*. These spherulitic growth rates are plotted for each composition as a function of the percentage of erucamide content in the blends (*Figure 9*). Spherulites of i-PP formed in blends clearly show a decrease in radial growth at 403, 404, 406, 408, 411 and 412 K as compared with that for pure i-PP, as it can be seen in *Figure 9*. Furthermore, the decrease reaches plateau values in the presence of very high amounts (about 30% and higher) of erucamide. The decrease found for i-PP spherulites grown from blends at 408, 411, and 412°C shows the same general pattern, but it is less pronounced.

Micrographs taken during crystallization of the blends show that for higher erucamide content they consist of two phases with erucamide domains embedded in the regions of i-PP spherulites. This gives the spherulites crystallized from the blends a grainy appearance. In higher erucamide content blends, the presence of two phases with big erucamide domains is very clearly seen. In these erucamide domains dispersed spherulitic groups which have not been grown in a homogeneous fashion can be very easily seen. They present an irregular non-flat border line. In some samples this border is somewhat dentated, and some others are incomplete and they seem to have been seized with the teeth.

Table 3 Spherulitic growth rate G for pure i-PP and i-PP in its blends with erucamide as a function of the crystallization temperature T_c and the percentage of erucamide content

	$G(T)$ (μm min^{-1})						
	Composition erucamide (wt%)						
T_c (K)	0	4	16	29	45	68	85
403	5.22	4.62	3.90	2.63	2.95	3.02	3.40
404	4.12	3.82	3.16	2.46	2.64	2.44	2.45
406	2.52	2.25	1.55	1.42	1.60	1.49	1.50
408	1.76	1.53	1.11	0.81	1.08	1.06	0.79
411	0.90	0.88	0.63	0.49	0.54	0.55	0.42
412	0.79	0.77	0.56	0.38	0.45	0.52	0.42

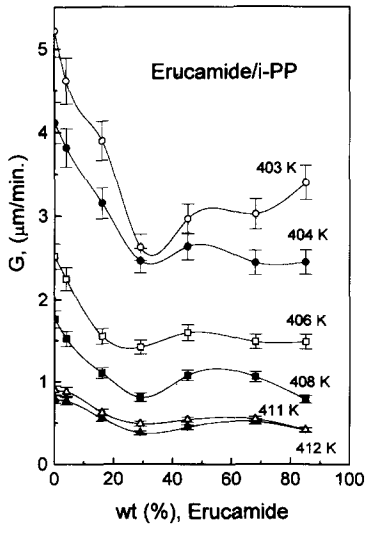

Figure 9 Plot of the spherulitic growth rate G as a function of the percentage of erucamide content in erucamide/i-PP blends at different crystallization temperatures

Scanning electron microscopy

Characteristic scanning electron microscopy (SEM) micrographs are given in *Figure 10*, showing that erucamide was poorly dispersed in i-PP. As can be seen in *Figure 10*, the sample with a 4% erucamide content does not show any erucamide globules. However, erucamide globules can be very easily observed in blends with higher erucamide contents (16% eru content). Particle sizes ranged from 0.3 to 10 μm depending on the blend composition. Poor interfacial adhesion was evident either from the large voids left on the fracture surface, where the particles had separated from the matrix, or from the smooth surfaces of the exposed erucamide particles. These morphologies are similar to those found by Valenza and Acierno[48] for the case of poly(propylene)/nylon 12 blends and by Valenza *et al.*[49] for poly(propylene)/nylon 6 blends.

DISCUSSION

The appearance of two quite well differentiated

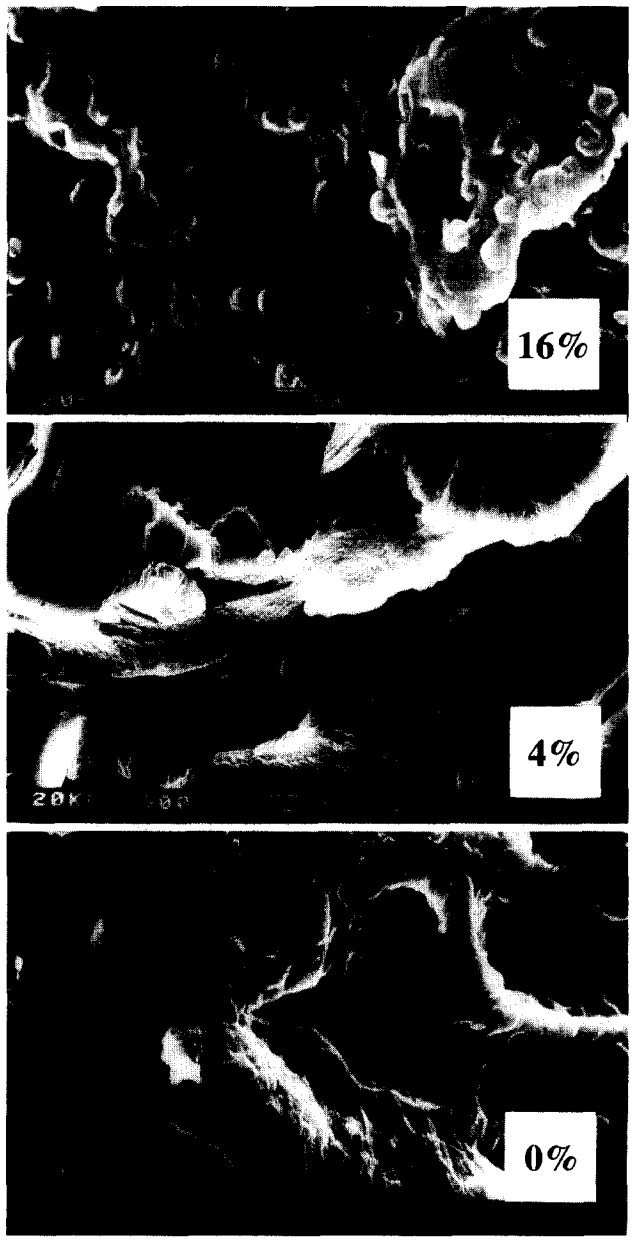

Figure 10 SEMs of room temperature fracture surface of a series of blends of erucamide/i-PP. Their compositions are indicated

endotherms in the d.s.c. trace for low erucamide content samples is probably due to the fact that a fraction of erucamide is located in the amorphous regions of spherulites and/or in their surroundings. In other words, this feature may be due to the crystallization of erucamide as microdomains. This erucamide melts at a different temperature. Such a behaviour is characteristic of substances crystallized within a matrix. We are going to assume that this type of erucamide corresponds to the endotherm appearing at the lower temperature, i.e. that which appears at 340 K. This means that the crystallinity exhibits dual-population melting behaviour for erucamide. Both endotherms present characteristic melting points and the relative areas of each of them has to be proportional to the erucamide content on the one hand, and to the i-PP amorphous content on the other. Both magnitudes are interrelated. These two endotherms are very easily distinguishable for blends of up to 29% erucamide content, but for blends with higher erucamide content they overlap and only one endotherm may be distinguishable, as is very easily seen in *Figure 1*. This peculiar behaviour deserves to be quantitatively analysed in detail later on.

The dependence found between the radial growth rate of i-PP spherulites in blends as a function of the percentage of erucamide composition in blends can be explained in the following terms. Bartczak *et al.*[19] have proposed a modified version of the Turnbull–Fisher equation to describe crystallization in immiscible blends. They introduce energy terms to account for the dissipation of energy due to the presence of a second phase. Their calculations show that the work done by the growing spherulites to reject the domains with a radius smaller than a certain critical size into the interlamellar regions is of greatest importance. As a consequence an energy loss occurs at the crystallization front, and a retardation in the radial growth rate results. This explanation is in agreement with the behaviour found in the present system. Although at this stage, i-PP and erucamide are already considered to be strictly incompatible, the inclusion of erucamide in the amorphous phase of the i-PP spherulites is not a function of the composition. It is necessary to take into account the amount of erucamide located in the amorphous zones of the spherulites as a function of the apparent melting enthalpy for each one of the blends.

At this point, let us discuss a model. Let us assume x as the erucamide content by weight per unit in any of the blends. Then $1 - x$ represents the respective i-PP content per unit of this blend. As we have seen before in *Table 1*, the degree of crystallinity of the i-PP remains almost constant all over the range of composition. Let us say about 56%. The precise value does not make any difference in our statement and arguments.

For a given sample the i-PP amorphous content will be therefore $1 - 0.56$, and therefore $(1 - x) \times (1 - 0.56)$ will represent the i-PP amorphous content in the blend. It is this amorphous fraction which we can consider as the amorphous region of the spherulites and/or the amorphous region surrounding the spherulites. However the amorphous regions are not completely occupied by erucamide crystals. Only a fraction is available to locate erucamide; let us call this fraction, F. Therefore, we can consider it as an adjustable parameter which represents the erucamide molecules within the amorphous regions of spherulites. The content of erucamide in these two amorphous regions, i.e. in and between spherulites in the blend, will be then expressed by $(1 - x) \times (1 - 0.56) \times F$. The proportion of erucamide in the amorphous phase of spherulites in relation to the whole content of erucamide may be expressed by $[(1 - x) \times (1 - 0.56) \times F]/x$, and if its apparent melting enthalpy is represented by ΔH_m (Erucamide II) i.e. erucamide in spherulites or simply $\Delta H_{ERU\,II}$, then the heat evolved due to erucamide located in the amorphous region in spherulites can be expressed as $[(1 - x) \times (1 - 0.56) \times F] \times \Delta H_{ERU\,II}/x$.

On the other hand, if $(1 - x) \times (1 - 0.56) \times F$ represents erucamide molecules located in the amorphous regions of spherulites (ERU II), $[x - (1 - x) \times (1 - 0.56) \times F]$ will represent the quantity of erucamide forming part of globules or droplets, and if its apparent melting enthalpy is represented by ΔH_m (ERU I), i.e. erucamide in globules, or simply $\Delta H_{ERU\,I}$, then $[x - (1 - x) \times (1 - 0.56) \times F] \times \Delta H_{ERU\,I}/x$ will represent the heat evolved due to erucamide in globules. Finally the whole enthalpy of melting of erucamide due to both contributions, i.e. from erucamide in spherulites and erucamide in globules, and after replacing ΔH_m (measured) by $\Delta H_{measured}$, it can finally be expressed by:

$$\Delta H_{measured} = \frac{(1 - x) \times (1 - 0.56) \times F \times \Delta H_{ERU\,II}}{x} + \frac{[x - (1 - x) \times (1 - 0.56) \times F] \times \Delta H_{ERU\,I}}{x} \quad (1)$$

This equation can be rearranged to:

$$\Delta H_{measured} = \frac{1 - x}{x} \times (1 - 0.56) \times F \times \Delta H_{ERU\,II} + \left[1 - \frac{1 - x}{x} \times (1 - 0.56) \times F\right] \times \Delta H_{ERU\,I} \quad (2)$$

for this expression when $x \to 1$, $\Delta H_{measured} \to \Delta H_{ERU\,I}$ (erucamide in globules or droplets) and when $x \to 0$, $\Delta H_{measured}$ must be equal to $\Delta H_{ERU\,II}$ (erucamide in spherulites, either as located in the amorphous region of spherulites and/or in the regions surrounding the

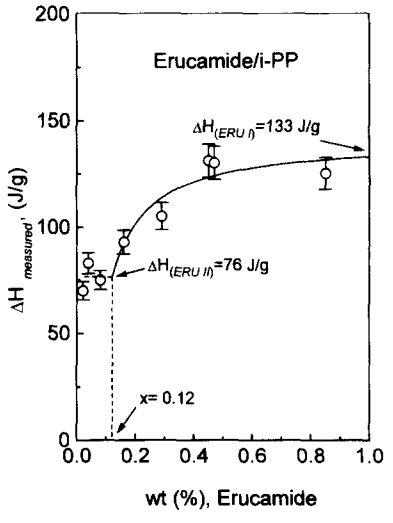

Figure 11 Apparent melting enthalpies $\Delta H_m = \Delta H_{measured}$ of erucamide and i-PP/erucamide blends as a function of erucamide content. The full line curve has been drawn, as explained in the text, by means of equation (1)

spherulites). However, it cannot be represented completely as described by the above equation, for the following reason. This expression is only true for erucamide content of $x > (1-x) \times (1-0.56) \times F$, namely, $x > 0.12$. In other words, the volume available in the amorphous region of the spherulites is higher than the volume of erucamide. A fraction of this volume is unoccupied by erucamide molecules. Let us say that it is an *empty available amorphous volume*.

In *Figure 11* is shown a plot of the experimental apparent melting enthalpy points represented by $\Delta H_{\text{measured}}$ against erucamide content x. The full line has been drawn by the best fitting method. The best fitting to the experimental data yields values for the parameters $\Delta H_{\text{ERU I}} = 133\,\text{J g}^{-1}$; $\Delta H_{\text{ERU II}} = 76\,\text{J g}^{-1}$ and $F = 0.3$. The values obtained for the two first parameters compare favourably well with the following experimentally obtained values of: ΔH_{m} (erucamide in spherulites, ERU II) $= 78.6\,\text{J g}^{-1}$, i.e. erucamide in and between the amorphous region of spherulites and ΔH_{m} (erucamide in globules, ERU I) $= 144.2\,\text{J g}^{-1}$. Furthermore, it has allowed us the estimation of the real percentage of amorphous regions occupied by erucamide, $F = 0.3$. As we can see, the agreement found between the theoretical curve which represents the model by the above equations (1) or (2), and the experimental result is fairly good.

However there may exist another possibility which must be ruled out. Let us assume, as a hypothesis, that we have only two types of different erucamide molecules, but both located in globules. In this case we may hypothetically have two possible types of erucamide molecules which would be distinguishable. One, which forms the bulk phase of the globule, and the other, forming part of the i-PP/erucamide interphase. Let us assume that this last one would present a different crystalline structure. This is only possible if we admit that an epitaxial growth of some other type of crystallization of erucamide crystals has taken place on the i-PP surface in a few layers with a structure quite different from that present in the bulk of the globules. In other words, the globules are recovered by pure erucamide, but with a crystalline structure quite well differentiated from that one in the core. In this case the quantity of every type of erucamide crystals will be directly related to the volume of the globule, and to the surface of the globule itself where they are enclosed, respectively. In both cases it would be necessary to have a direct relation between the volume and surface area of globules, which would represent approximately these two possible types of well differentiated crystalline structures of erucamide. This does not seem to be the case, as can be very easily deduced from our experimental results, especially for samples with a low percentage of erucamide. In addition, SEM microphotographs obtained with a magnification of 1.5×10^4 on samples with a low content of erucamide do not show any appreciable sign of globules. This means that for these low percentages the second type of erucamide crystals must be located in the amorphous region of spherulites.

Further WAXS and SAXS investigations, to determine the crystalline structure of erucamide in the amorphous regions and the interphase distribution function of erucamide in the i-PP matrix and/or the interphase between spherulites, are currently being performed.

CONCLUSIONS

1. A single glass transition for the blend which does not vary with composition is observed, suggesting that the components are incompatible in the range of blending studied. The work reported in the present paper also shows the incompatibility between the additive dispersed in the polymeric matrix as a whole, and in the amorphous regions of spherulites and/or between the amorphous surrounding regions of spherulites and that the phenomenon of incompatibility is also related to the volume fraction in the amorphous phase of the matrix (degree of crystallinity).
2. A relationship has been established, via d.s.c. measurements, which permits a quantitative description between the degree of dispersion of the additive in the amorphous part of the i-PP spherulites and/or the regions (Erucamide II) which surround the spherulites and the excess of additive which forms a separated phase as globules or droplets inside the polymeric matrix (Erucamide I).
3. The univoque existence of this second type of (Erucamide II) has been tested by means of blends prepared by diffusion of erucamide in i-PP films as well as by immersion of i-PP films in melt erucamide. In both cases erucamide must be located in the amorphous regions of spherulites and/or in the amorphous regions surrounding the spherulites, and never as globules or droplets in the polymeric matrix, since these are only formed by dry melt blending of erucamide and i-PP.
4. The crystallization kinetics of i-PP have been followed by optical microscopy. A decrease of the radial growth rate for i-PP spherulites grown from the melt of blends was observed. The morphology of these spherulites appears to be identical to those grown from pure i-PP. In other words, either the addition of erucamide at a fixed T_c or the increase of T_c at a fixed i-PP concentration reduced the crystallization rate. Immiscibility offers a logical explanation for the observed behaviour.

ACKNOWLEDGEMENTS

The authors are indebted, and express their thanks to the following. To Dr A. Bisbal from DISPER, S. A., San Andreu de la Barca (Barcelona), for kindly providing the Hostalen PPN 1060 sample of free-additives propylene film, which was prepared especially to carry out the present series of experiments. Special thanks are given to Dr J. M. Palacios Latasa and Mrs Loreto Bajón Román of the Departamento de Microscopía Electrónica at the Instituto de Catálisis y Petroleoquímica del C.S.I.C. (Tres Cantos, Madrid) for SEM microphotographs. One of us (I. Q.-G.) thanks the Consejería de Educación of the Communidad de Madred for a Beca de Formación del personal Investigador y Técnico of the Plan Regional de Investigación. This work was partially supported by the DCICYT through Grant PB 92-0773-03-1 and the CICYT Project MAT 94-0858-E.

REFERENCES

1. Glover, J. H., *Rev. Tappi J.*, 1988, **71**, 188.
2. Billingham, N. C., *Makromol. Chem., Macromol. Symp.*, 1989, **27**, 187.

3. Quijada-Garrido, I., Barrales-Rienda, J. M. and Frutos, G., *Macromolecules*, 1996, **29**, 7164.
4. Molnar, N. M., *J. Am. Oil Chem. Soc.*, 1974, **51**, 84.
5. Peterlin, A., *J. Macromol. Sci.*, 1975, **B11**, 57.
6. Billingham, N. C., in *Oxidation Inhibition in Organic Materials*, Vol. 2, ed. P. Pospisil and P. P. Klemchuck. CRC Press, Boca Raton, FL, 1990, Chap. 6, p. 249.
7. Hildebrand, J. H. and Scott, R. L., *The Solubility of Nonelectrolytes*, 3rd Edn. Reinhold, New York, 1950.
8. Stannett, V. and Yasuda, H., in *Crystalline Olefin Polymers*, Part II, ed. R. A. V. Raff and K. W. Doak. Interscience, New York, 1964, Chap. 4, p. 131.
9. Földes, E., *Polym. Deg. Est.*, 1995, **49**, 57.
10. Wlochowicz, A., Broda, J. and Slusarczyk, C., *Acta Polymerica*, 1989, **40**, 95.
11. Wlochowicz, A. and Broda, J., *J. Appl. Cryst.*, 1991, **24**, 715.
12. Wlochowicz, A. and Broda, J., *J. Polym. Eng.*, 1991, **10**, 71.
13. Wlochowicz, A. and Garbarczyk, J., *Polym. Int.*, 1994, **34**, 253.
14. Mandelkern, L., *Crystallization of Polymers*. McGraw-Hill, New York, 1964.
15. Lim, G. B. A. and Lloyd, D. R., *Polym. Eng. Sci.*, 1993, **33**, 522.
16. Quijada-Garrido, I., Barrales-Rienda, J. M., Pereña, J. M. and Frutos, G., *J. Polym. Sci., Polym. Phys. Edn*, accepted for publication.
17. Kishore, K. and Vasanthakumari, R., *Polymer*, 1986, **27**, 337.
18. Martuscelli, E., *Polym. Eng. Sci.*, 1984, **24**, 563.
19. Bartczak, Z., Galeski, A. and Martuscelli, E., *Polym. Eng. Sci.*, 1984, **24**, 1155.
20. Chatterjee, A. M., Price, F. P. and Newman, S., *J. Polym. Sci., Polym. Phys. Edn*, 1975, **13**, 2369, 2385, 2391.
21. Aref-Aqzar, A., Hay, J. N., Marsden, B. J. and Walker, N., *J. Poly. Sci., Polym. Phys. Edn*, 1980, **18**, 637.
22. Ghijsels, A., Groesbeek, N. and Yip, C. W., *Polymer*, 1982, **23**, 1913.
23. Robitaille, C. and Prud'homme, J., *Macromolecules*, 1983, **16**, 665.
24. Tang, T. and Huang, B., *J. Appl. Polym. Sci.*, 1994, **53**, 355.
25. Brengartner, D. A., *J. Am. Oil. Chem. Soc.*, 1986, **63**, 1340.
26. Miller, R. L., in *Encyclopedia of Polymer Science and Technology. Plastics, Resins, Rubbers, Fibers*, Vol. 4, ed. H. F. Mark, N. G. Gaylord and N. Bikales. John Wiley, New York, 1966, pp. 449–528.
27. Van Krevelen, D. W., *Properties of Polymers*, Elsevier, Amsterdam, 1976.
28. Barrales-Rienda, J. M., González Ramos, J. and Sánchez Chaves, M., *Br. Polym. J.*, 1977, **9**, 6.
29. St Jean, G., Barreto, M. C. and Brown, G. R., *Polym. Eng. Sci.*, 1990, **30**, 1098.
30. Frutos, G., Quijada, I. and Barrales-Rienda, J. M., *Analyst*, 1994, **119**, 1547.
31. Frank, H. P. and Lehner, H., *J. Polym. Sci., Part C*, 1970, **31**, 193.
32. Curson, A. D., *Proc. Royal Microsc. Soc.*, 1972, **7**, 96.
33. Billingham, N. C., Calvert, P. D., Prentice, P. and Ryan, T. G., *Polym. Preprints, Am. Chem. Soc., Polym. Chem. Div.*, 1977, **18**, 476.
34. Calvert, P. D. and Ryan, T. G., *Polymer*, 1978, **19**, 611.
35. Billingham, N. C. and Calvert, P. D., *Developments in Polymer Stabilization*, 1980, **3**, 139.
36. Martuscelli, E., Canetti, M. and Seves, A., *Polymer*, 1989, **30**, 304.
37. Wenig, W. and Fiedel, H.-W., *Makromol. Chem.*, 1991, **192**, 85.
38. Wenig, W. and Wasiak, A., *Colloid Polym. Sci.*, 1993, **271**, 824.
39. Unpublished results.
40. Mandelkern, L., *J. Appl. Polym. Sci.*, 1955, **26**, 443.
41. Boon, J. and Azcue, J. M., *J. Polym. Sci.*, 1968, **6**, 885.
42. Wang, Y. F. and Lloyd, D. R., *Polymer*, 1993, **34**, 4740.
43. Okada, T., Saito, H. and Inoue, T., *Polymer*, 1993, **34**, 4752.
44. Chatuverdi, P. N., *Makromol. Chem.*, 1987, **188**, 433.
45. Keith, H. D. and Padden, F. J., *J. Appl. Phys.*, 1964, **35**, 1270.
46. Keith, H. D. and Padden, F. J., *J. Appl. Phys.*, 1964, **35**, 1286.
47. Keith, H. D. and Padden, F. J., *J. Appl. Phys.*, 1964, **34**, 2409.
48. Valenza, A. and Acierno, D., *Eur. Polym. J.*, 1994, **30**, 1121.
49. Valenza, A., La Mantia, F. P., Demma, G. B., Romano, V. and Acierno, D., *Polym. Networks Blends*, 1991, **1**, 71.